

## A theoretical study of the carbenoids $\text{LiCH}_2\text{X}$ ( $\text{X} = \text{Cl}, \text{Br}, \text{I}$ ) cyclopropanation reaction with ketene

XING HUI ZHANG<sup>1,\*</sup>, FU LONG ZHANG<sup>1</sup> and ZHI YUAN GENG<sup>2</sup>

<sup>1</sup>College of Chemical Engineering, Gansu Lianhe University, Lanzhou 730010, P.R. China

<sup>2</sup>College of Chemistry and Chemical Engineering, Northwest Normal University, Lanzhou 730070, P.R. China

e-mail: zhxh135@126.com

MS received 4 May 2009; revised 18 January 2010; accepted 22 January 2010

**Abstract.** A computational study for the [2 + 1] addition of the lithium carbenoids  $\text{LiCH}_2\text{X}$  ( $\text{X} = \text{Cl}, \text{Br}, \text{I}$ ) with ketene have been investigated by means of the B3LYP hybrid density functional method. All the reactions examined displayed similar concerted mechanisms for the cyclopropanation of these reagents. The lithium carbenoids react with ketene via an asynchronous attack on one  $\text{CH}_2$  or C group of ketene with relatively low barrier to reaction in the range of 25.34–33.74 kJ/mol in THF solvent. The trend of the lithium carbenoids reaction barrier with ketene is  $\text{LiCH}_2\text{Cl} < \text{LiCH}_2\text{Br} < \text{LiCH}_2\text{I}$ . The results show that the reactions could be highly chemical reactivity with low barriers and could be favoured in experiment. The reactions could proceed easily at lower temperature. The computational results are briefly compared to other carbenoid reactions and related species.

**Keywords.** Density functional theory; ketene; lithium carbenoid.

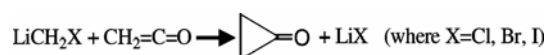
### 1. Introduction

Cyclopropane-containing molecules are found in a wide range of natural and unnatural compounds that display important biological activities and in many substances used as starting materials and intermediates in organic synthesis.<sup>1–14</sup> Since the reported use of diiodomethane and a Zn/Cu couple to react with olefins to form cyclopropane units by Simmons and Smith.<sup>15</sup> This has motivated a large number of research groups to develop new and wide-range methods to produce cyclopropanated products. Methylene insertion by a carbenoid species into the C=C bond is one of the most widely used methods since the recognition of the Simmons–Smith reaction, which is a reaction between iodomethylzinc iodide and an olefin that produces a cyclopropane compound was first reported by Simmons and Smith in 1958.<sup>16</sup> Following a great deal of work has been done to improve and develop alternative methods to produce Simmons–Smith-type reagents. Many researchers have been trying to find more efficient and highly diastereoselective cyclopropanating reagents. In 1964, Closs and Moss<sup>17</sup> discovered a

lithium carbenoid that can give the expected arylcyclopropanes in the presence of olefins at  $-10^\circ\text{C}$  with moderate to good yields.

In this paper, we carried out the calculations on  $\text{LiCH}_2\text{X}$  (where  $\text{X} = \text{Cl}, \text{Br}, \text{I}$ ) carbenoids promoted cyclopropanation reactions with ketene investigated using theoretical methods. As expected for ‘carbenoids’,  $\text{LiCH}_2\text{X}$ , X is the electrophilic behaviour of these species: the methylene of  $\text{LiCH}_2\text{X}$  adds to C=C double bonds of ketene to produce cyclopropanone, see scheme 1.

These computational results are good forecast for the experimental results, and the mechanisms of the title reaction are mainly discussed. The  $\text{LiCH}_2\text{Cl}$  carbenoid (reaction barrier of  $< 25.73$  kJ/mol) is found to be the most reactive carbenoid in the  $\text{LiCH}_2\text{X}$  ( $\text{X} = \text{Cl}, \text{Br}, \text{I}$ ) series of carbenoids and the  $\text{LiCH}_2\text{I}$  carbenoid is the least reactive one. But it is one of the most widely used X type of the carbenoids. We compare our present results for the lithium



**Scheme 1.** Cyclopropanation reactions of ketene with carbenoids  $\text{LiCH}_2\text{X}$ .

\*For correspondence

carbenoids promoted cyclopropanation reactions in relation to other metal carbenoid reactions<sup>18–31</sup> and experimental results.

## 2. Computational details

The hybrid B3LYP density functional method<sup>32,33</sup> was used to investigate the cyclopropanation reaction mechanisms of the lithium carbenoids with ketene. The geometries of all stationary points (reactants, transition states and products) were fully optimized at the B3LYP level of theory. The analytical frequency calculations at the same level of theory were performed to confirm the characters of optimized structures and to obtain zero-point energy corrections. Furthermore, intrinsic reaction coordinate (IRC) calculations<sup>34</sup> were performed to confirm the optimized transition state correctly connecting related reactants and products. Geometry optimization and frequency calculations were carried out with the 6-311++G\*\* basis set for all Li, C, H, and the LANL2DZ basis set for halogen atoms. To consider solvent effects on the reactions of interest, the polarized continuum model (PCM)<sup>35,36</sup> was applied to the calculations. Single-point energy calculations

were done at the B3LYP/PCM/6-311++G\*\* level of theory. All calculations were carried out using the Gaussian 98 program suite.<sup>37</sup>

## 3. Results and discussion

The optimized stationary structures (minima and saddle points) on the potential energy surfaces of the reactions are depicted schematically in figures 1–3. Selected key geometry parameters (bond lengths and bond angles) for these structures are also given in figures 1–3 and table 1. The total energies with ZPE correction, the relative energy of starting molecules and vibration frequencies are listed in table 2.

The optimized geometry for the  $\text{LiCH}_2\text{Cl}$  is shown in figure 1 along with the optimized geometry of the reactants and the transition states (TS1, TS2) for cyclopropanations of ketene through two different pathways to produce cyclopropanone ( $c\text{-C}_3\text{H}_4$ )=O and LiCl. A weak complex may be formed when the two molecules move toward one another, but this has little effect on the chemical reaction. The pathways involve concerted [2 + 1] addition mechanism through the three-centered transition states (TS1, TS2), in which the pseudotrigonal

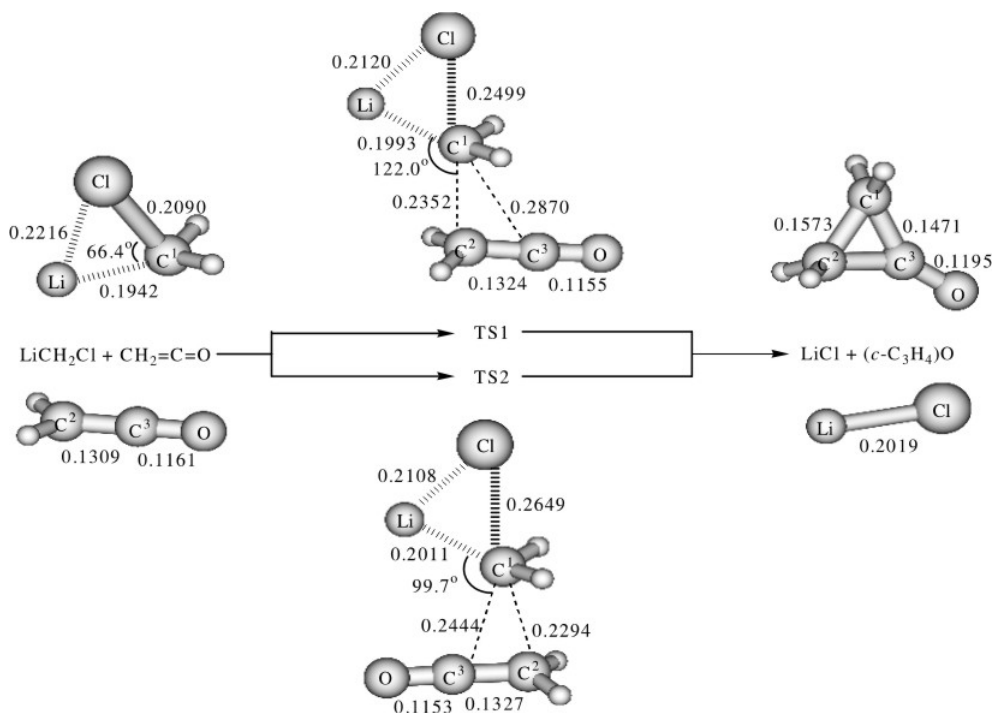


**Figure 1.** Schematic diagrams of the optimized geometry from the B3LYP/6-311++G\*\* computations for the reactions of  $\text{LiCH}_2\text{Cl}$  with ketene. Selected structural parameters are shown for each species with the bond lengths in nm and the bond angles in deg.

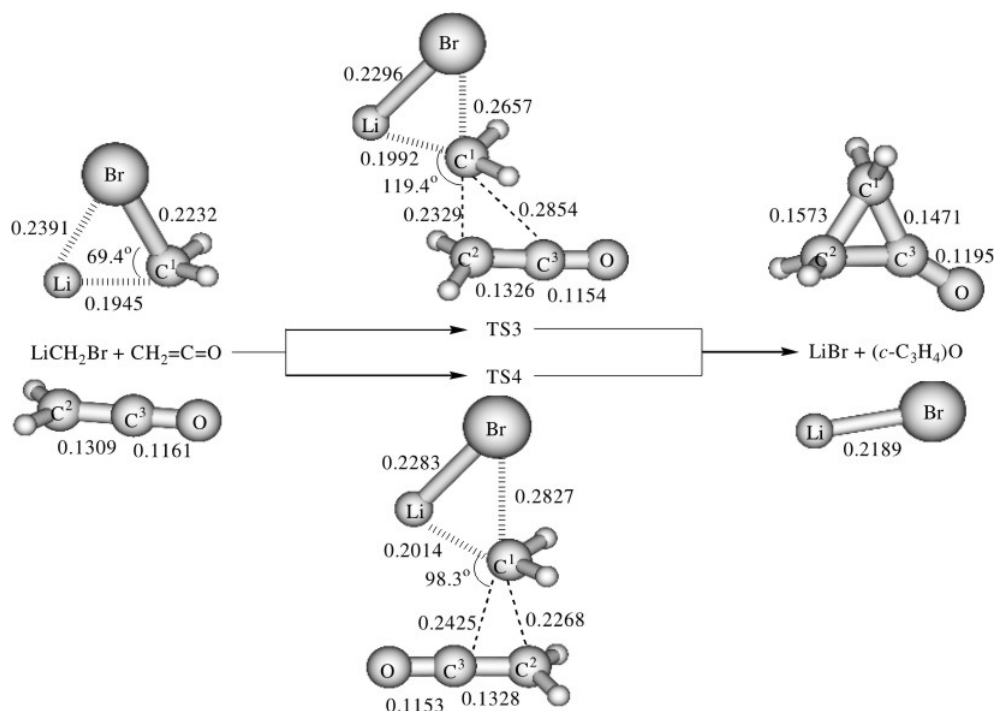


**Figure 2.** Schematic diagrams of the optimized geometry from the B3LYP/6-311++G\*\* computations for the reactions of  $\text{LiCH}_2\text{Br}$  with ketene. Selected structural parameters are shown for each species with the bond lengths in nm and the bond angles in deg.

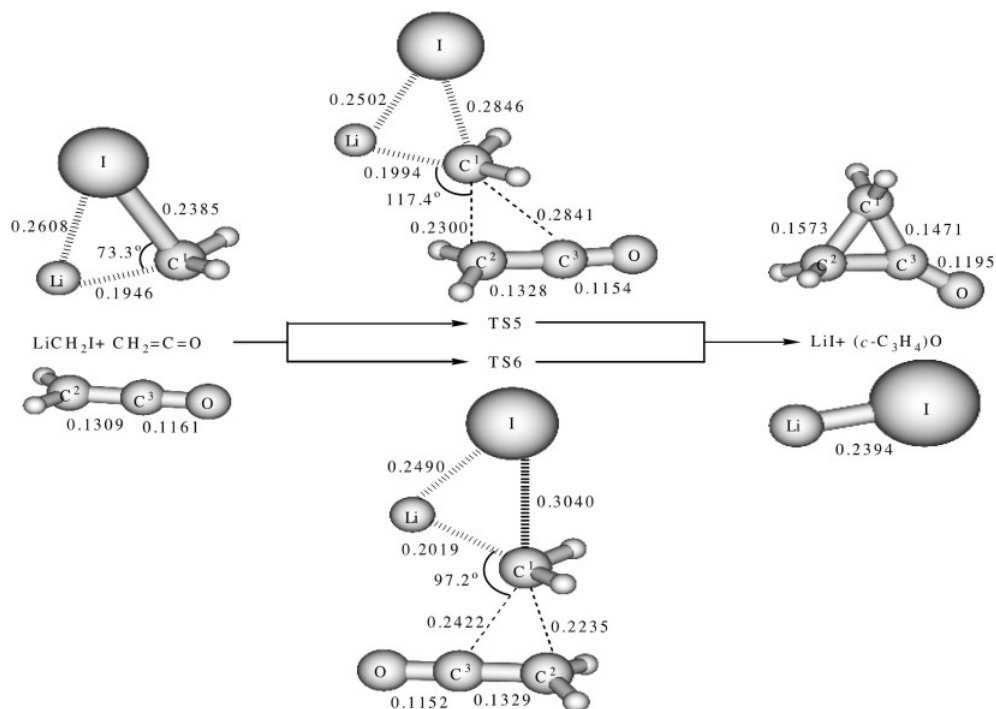


**Figure 3.** Schematic diagrams of the optimized geometry from the B3LYP/6-311++G\*\* computations for the reactions of  $\text{LiCH}_2\text{I}$  with ketene. Selected structural parameters are shown for each species with the bond lengths in nm and the bond angles in deg.

**Table 1.** Calculated bond lengths and bond elongation in the TS $n$  ( $n = 1-6$ ) as compared to the bond lengths of the starting materials (LiCH $_2$ X, where X = Cl, Br, I), respectively.

X	TS $n$	C <sup>1</sup> -Li $r$ (nm)	C <sup>1</sup> -Li elong. (%)	C <sup>1</sup> -X $r$ (nm)	C <sup>1</sup> -X elong. (%)	Li-X $r$ (nm)	Li-X elong. (%)
Cl	TS1	0.1993	2.63	0.2499	19.57	0.2120	-4.33
Cl	TS2	0.2011	3.55	0.2649	26.75	0.2108	-4.87
Br	TS3	0.1992	2.42	0.2657	19.04	0.2296	-3.97
Br	TS4	0.2014	3.55	0.2827	26.66	0.2283	-4.52
I	TS5	0.1994	2.47	0.2846	19.33	0.2502	-4.06
I	TS6	0.2019	3.75	0.3040	27.46	0.2490	-4.52

**Table 2.** Total energies with ZPE correction ( $E_t$ ), relative energies ( $E_r$ ), and vibration frequencies ( $\nu$ ) of the geometries.

System	Gas-phase $E_t$ /a.u.	Gas-phase $E_r$ /(kJ · mol <sup>-1</sup> )	THF $E_t$ /a.u.	THF $E_r$ /(kJ · mol <sup>-1</sup> )	$\nu$ /cm <sup>-1</sup>
LiCH $_2$ Cl + CH $_2$ =C=O	-214.37607	0.00	-214.47591	0.00	-
LiCH $_2$ Br + CH $_2$ =C=O	-212.59502	0.00	-212.69408	0.00	-
LiCH $_2$ I + CH $_2$ =C=O	-210.81427	0.00	-210.91283	0.00	-
TS1	-214.36941	17.49	-214.46626	25.34	253.34 <i>i</i>
TS2	-214.36945	17.38	-214.46611	25.73	271.18 <i>i</i>
TS3	-212.58724	20.43	-212.68377	27.07	263.83 <i>i</i>
TS4	-212.58700	21.06	-212.68372	27.20	279.96 <i>i</i>
TS5	-210.80464	25.28	-210.90106	30.90	278.24 <i>i</i>
TS6	-210.80394	27.12	-210.89998	33.74	291.01 <i>i</i>
LiCl + ( <i>c</i> -C $_3$ H $_4$ )O	-214.43399	-152.07	-214.57017	-247.48	-
LiBr + ( <i>c</i> -C $_3$ H $_4$ )O	-212.64878	-141.15	-212.78581	-240.84	-
LiI + ( <i>c</i> -C $_3$ H $_4$ )O	-210.86326	-128.62	-210.81756	-250.13	-

methylene group of the carbenoid adds to the C=C  $\pi$ -bond of ketene to form two new C-C bonds asynchronously. As shown in figure 1, The C<sup>1</sup>-Cl, Li-Cl and Li-C<sup>1</sup> bond lengths are 0.2090, 0.2216 and 0.1942 nm in the structure of LiCH $_2$ Cl, respectively. The three-centered transition structures TS1 and TS2 are formed easily when the two molecules (LiCH $_2$ Cl and CH $_2$ =C=O) move toward one another. The C $_1$ -C $_2$  bond lengths in TS1 and TS2 are 0.2352 and 0.2294 nm and this is 0.0518 and 0.0150 nm shorter than the C $_1$ -C $_3$  distance, respectively. This indicates a concerted asynchronous pathway for the cyclopropanation reaction of LiCH $_2$ Cl with ketene. The relatively large C $_1$ -C $_2$  and C $_1$ -C $_3$  distances predict that TS1 is closer to the reactants in structure than the products. The C<sup>1</sup>-Cl and Li-C<sup>1</sup> distances are elongated by 19.57–26.75% and 2.63–3.55% from the reactants to TS1 and TS2, respectively (table 1). However, the Li-Cl bond lengths shortened by 4.33–4.87% from the reactants to TS1 and TS2. Notably, in the transition state TS1 and TS2, the C<sup>1</sup>-Cl bonds become nearly broken and the electron-rich Cl atom is attracted by the metal center to

result in an almost complete Li-Cl bond. These changes in the bond lengths are attributed to partial formation of the LiCl by-product in the transition state. The planar ketene molecule has a significant pyramidalization of about 6.7° for C2 in TS1 and this indicates the onset of the  $sp^2 \rightarrow sp^3$  rehybridization required. It is evident that TS1 and TS2 are the transition states of the concerted reaction from LiCH $_2$ Cl + CH $_2$ CO reactants to (*c*-C $_3$ H $_4$ )O + LiCl products. Vibrational analysis shows that the TS1 and TS2 structures have one imaginary frequency of 253.34*i* cm<sup>-1</sup> and 271.18*i* cm<sup>-1</sup>, respectively. The transition states were confirmed to be the first-order saddle point connecting the corresponding reactants and products by IRC calculations.

To obtain more reliable data, the solvent (THF,  $\epsilon = 7.58$ ) effect through PCM calculations has been considered at B3LYP/PCM/ 6-311++G\*\* for the reaction species. The results confirm the same trends which indicate that the energy difference does not reveal a significant change (7.85–8.35 kJ/mol). As far as the two activation energies ( $E_r$ ) with ZPE correction computed for TS1 and TS2 are concerned,

the two pathways of TS1 and TS2 have the low-energy barriers of 25.34 and 25.73 kJ/mol respectively and is exothermic by about 247.48 kJ/mol in THF solvent at the B3LYP level of theory (table 2). From the kinetic point of view, the carbenoid  $\text{LiCH}_2\text{Cl}$  should be overcome easily for TS1 and TS2 to product cyclopropanone.

To further improve our understanding of the reaction activity about different lithium carbenoids, we carried out calculations on changing the Cl atom to a Br or I atom in the  $\text{LiCH}_2\text{Cl}$  carbenoid lead to formation of the  $\text{LiCH}_2\text{Br}$  and  $\text{LiCH}_2\text{I}$  carbenoids, respectively. The similar reaction pathways have been determined. The transition states TS3 (263.831  $\text{cm}^{-1}$ ), TS4 (279.961  $\text{cm}^{-1}$ ), TS5 (278.241  $\text{cm}^{-1}$ ) and TS6 (291.011  $\text{cm}^{-1}$ ) were found for the reactions of  $\text{LiCH}_2\text{Br}$  and  $\text{LiCH}_2\text{I}$  with ketene to cyclopropanone and  $\text{LiBr}$  and  $\text{LiI}$  products, respectively. The geometry of TS3 and TS5 are similar to that of TS1. The reaction has a barrier of 27.07 and 30.90 kJ/mol and is exothermic by about 240.84 and 250.13 kJ/mol at the B3LYP/6-311++G\*\* level of theory, respectively, as shown in table 2. The geometry of TS4 and TS6 are similar to that of TS2 and the reaction has a barrier height of 27.30 and 33.74 kJ/mol. As shown in table 2 and figure 4, compared to the reaction of  $\text{LiCH}_2\text{Cl} + \text{CH}_2=\text{C}=\text{O}$ , the reaction barrier of  $\text{LiCH}_2\text{Br} + \text{CH}_2=\text{C}=\text{O}$  becomes slightly higher by 1.73 kJ/mol while the exothermicity of the reaction becomes smaller by 6.64 kJ/mol. The reaction barrier of  $\text{LiCH}_2\text{I} +$

$\text{CH}_2=\text{C}=\text{O}$  becomes higher by 5.56 kJ/mol and the exothermicity of the reaction becomes higher by 2.65 kJ/mol than the reaction of  $\text{LiCH}_2\text{Cl} + \text{CH}_2=\text{C}=\text{O}$ . The trend of the lithium carbenoids reaction reactivity is  $\text{LiCH}_2\text{Cl} > \text{LiCH}_2\text{Br} > \text{LiCH}_2\text{I}$ . Figure 4 shows the reaction channels of TS1, TS3 and TS5 proceed much more easily than that of TS2, TS4 and TS6, respectively. The relatively low barriers for the two pathways can mainly be attributed to the following two reasons. First, there are only relatively small structural changes for the reactants to the transition states. Second, the lithium carbenoids have strong electrophilic character. However, the transition states TS2, TS4 and TS6 have higher energy because of sterically hindered effect.

As seen in figures 1–3 and table 1, the three-centered transition states TS (1, 3, 5) and TS (2, 4, 6) have several common features, respectively. For instance, The  $\text{C}^1\text{-X}$  ( $X = \text{Cl, Br, I}$ ) bonds are mostly broken in TS1-6 and the  $\text{C}^1\text{-Li}$  bonds are only slightly elongated compared with those of the reactants. Table 1 lists  $\text{C}^1\text{-Li}$ ,  $\text{C}^1\text{-X}$  and  $\text{Li-X}$  bond lengths as well as differences in bond lengths [%] in the transition states as compared to those in starting materials. The  $\text{C}^1\text{-X}$  bond is strongly elongated and the  $\text{C}^1\text{-X}$  ( $X = \text{Cl, Br, I}$ ) bonds are elongated by 19.57–26.75%, 19.04–26.66%, and 19.33–27.46%, respectively. Similarly, the  $\text{Li-C}^1$  bonds are elongated by 2.42–3.75% from the reactants to TS1-6. However, the  $\text{Li-X}$  bonds are slightly shortened in the transition states, and the stronger  $\text{Li-X}$  interaction can give sufficient compensation for the weakening of the  $\text{Li-C}^1$  bond from the reactants to TS. These results can explain why the  $\text{LiCH}_2\text{Cl}$  carbenoid is the most reactive of the  $\text{LiCH}_2\text{X}$  ( $X = \text{Cl, Br, I}$ ) carbenoids and these changes in the bond lengths are attributed to partial formation of the  $\text{LiCl}$  by-product in TS.

In recent years, many research groups have reported experimental and theoretical investigations for the reaction mechanisms of carbenoid-promoted cyclopropanation reactions. As for lithium carbenoids, Hermann *et al*<sup>25</sup> observed feasible reaction pathways and supported those using computational methods. MP2/6-311++G\*\* calculations predicted a barrier of 29.40 kJ/mol. The reaction barrier computed for the reaction of  $\text{ISmCH}_2\text{I}$  with  $\text{CH}_2\text{CH}_2$  is 36.78 kJ/mol.<sup>30</sup> The barriers for the reactions of the  $\text{EtZnCHI}_2$  and  $\text{IZnCHI}_2$  carbenoids<sup>28</sup> with ethylene are reported to be 83.60 and 102.41 kJ/mol, respectively. The aluminum carbenoid<sup>27</sup> has a barrier of 53.76 kJ/mol and we observed that the barrier heights

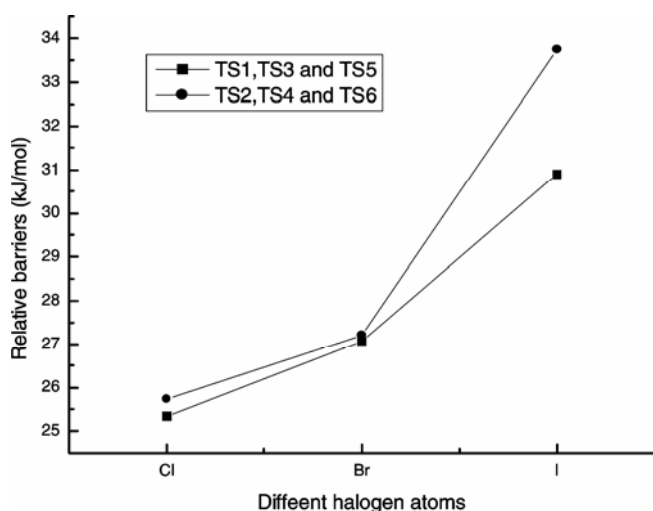


**Figure 4.** Barriers to the reaction calculated from the starting materials to the transition states for the reaction of  $\text{LiCH}_2\text{X}$  ( $X = \text{Cl, Br, I}$ ) with ketene as a function of different halogen atoms in THF solvent.

for the reactions increase in the following order, with computed barrier heights given in parentheses:  $\text{LiCH}_2\text{I} \approx \text{ISmCH}_2\text{I} < (\text{CH}_3)_2\text{AlCH}_2\text{I} < \text{IZnCH}_2\text{I}$ . Moreover, these reactions are in reasonable agreement with experimental reaction conditions showing that the cyclopropanation reaction can take place at low temperatures. Lithium and samarium carbenoids are the most reactive cyclopropanation reagents, and they can cyclopropanate olefins at  $-78^\circ\text{C}$ . Our studies indicate that the reaction for the lithium carbenoids  $\text{LiCH}_2\text{X}$  ( $\text{X} = \text{Cl}, \text{Br}, \text{I}$ ) with ketene have barriers of 25.34–33.74 kJ/mol in THF solvent at the B3LYP/6-311++G\*\* level of theory. These results predict that the reactions are likely to take place easily to produce cyclopropanone in experiment.<sup>25</sup> The above comparison is qualitatively consistent with the experimental reaction conditions and helps to provide a reasonable explanation for understanding the reactivity of these reactions.

#### 4. Conclusion

In this paper, density functional theory calculations have been presented for the reaction mechanisms of  $\text{LiCH}_2\text{X}$  ( $\text{X} = \text{Cl}, \text{Br}, \text{I}$ ) with ketene at the B3LYP level of theory. All the reactions proceed with the three-centered transition states to produce cyclopropanone and  $\text{LiX}$  ( $\text{X} = \text{Cl}, \text{Br}, \text{I}$ ). The barriers for system reactions stayed relatively low of 25.34–33.74 kJ/mol range and were strongly exothermic in THF solvent. A brief comparison of the lithium carbenoids and the other carbenoid species has shown that the lithium carbenoids have highly chemical reactivity to produce cyclopropanone. The computed results predict that the reactions could take place at low temperatures.

#### Supporting information

Tables of Cartesian coordinates, total energies and vibrational zero-point energies for all carbenoid reactants, transition states and products reported in this paper (table S1). See [www.ias.ac.in/chemsci](http://www.ias.ac.in/chemsci) for supporting information.

#### References

- Rappoport Z (ed) 1987 *The chemistry of the cyclopropyl group* (Chichester, UK: Wiley)
- Fritschi H, Leutenegger U and Pfaltz A 1986 *Angew. Chem. Int. Ed. Engl.* **25** 1005
- Evans D A, Woerpel K A, Hinman M M and Faul M M 1991 *J. Am. Chem. Soc.* **113** 726
- Rodriguez J B, Marquez V E, Nicklaus M C and Barchi J 1993 *Tetrahedron Lett.* **34** 6233
- Zhao Y, Yang T F, Lee M, Chun B K, Du J, Schinazi R F, Lee D, Newton M G and Chu C K 1994 *Tetrahedron Lett.* **35** 5405
- Nishiyama H, Itoh Y, Matsumoto H, Park S B and Itoh K 1994 *J. Am. Chem. Soc.* **116** 2223
- Doyle M P 1995 In *Comprehensive Organometallic Chemistry II* (ed.) L S Hegeudus (Oxford, UK: Pergamon) Vol. 12
- Nishiyama H, Itoh Y, Sugawara Y, Matsumoto H, Aoki K and Itoh K 1995 *Bull. Chem. Soc. Jpn.* **68** 1247
- Nishiyama H, Aoki K, Itoh H, Iwamura T, Sakata N, Kurihara O and Motoyama Y 1996 *Chem. Lett.* **25** 1071
- Doyle M P, McKerverey M A and Ye T 1998 *Modern catalytic methods for organic synthesis with Diazo compounds* (New York: Wiley)
- Boger D L, Ledebor M W, Kume M and Jin Q 1999 *Angew. Chem. Int. Ed.* **38** 2424
- Salaun J 2000 In *Small ring compounds in organic synthesis, VI* (ed.) A Meijere (Berlin: Springer), Vol. 207, pp. 1–67
- Che C M, Huang J S, Lee F W, Li Y, Lai T S, Kwong H L, Teng P F, Lee W S, Lo W C, Peng S M and Zhou Z Y 2001 *J. Am. Chem. Soc.* **123** 4119
- Rodriguez-Garcia C, Oliva A, Ortuno R M and Branchadell V 2001 *J. Am. Chem. Soc.* **123** 6157
- Simmons H E and Smith R D 1959 *J. Am. Chem. Soc.* **81** 4256
- Simmons H E and Smith R D 1958 *J. Am. Chem. Soc.* **80** 5323
- Closs G L and Moss R A 1964 *J. Am. Chem. Soc.* **86** 4042
- Maruoka K, Fukutani Y and Yamamoto H 1985 *J. Org. Chem.* **50** 4412
- Molander G A, Etter J B and Zinke P W 1987 *J. Am. Chem. Soc.* **109** 453
- Molander G A and Harring L S 1989 *J. Org. Chem.* **54** 3525
- Charette A B and Beauchemin A 2001 *J. Organometallic Chem.* **617** 702
- Bernardi F, Bottoni A and Miscione P 1997 *J. Am. Chem. Soc.* **119** 12300
- Dargel T K and Koch W 1996 *J. Chem. Soc. Perkin-Trans.* **2** 877
- Nakamura M, Hirai A and Nakamura E 2003 *J. Am. Chem. Soc.* **125** 2341
- Hermann H, Lohrenz J C W, Kuhn A and Boche G 2000 *Tetrahedron.* **56** 4109
- Fang W H, Phillips D L, Wang D and Li Y L 2002 *J. Org. Chem.* **67** 154
- Li Z H, Ke Z F and Zhao C Y 2006 *Organometallics* **25** 3735
- Zhao C Y, Wang D and Phillips D L 2002 *J. Am. Chem. Soc.* **124** 12903
- Stiasny H C and Hoffman R W 1995 *Chem. Eur. J.* **1** 619

30. Zhao C Y, Wang D and Phillips D L 2003 *J. Am. Chem. Soc.* **125** 15200
31. Wang D, Zhao C Y and Phillips D L 2004 *J. Org. Chem.* **69** 5512
32. Becke A D 1993 *J. Chem. Phys.* **98** 5648
33. Lee C, Yang W and Parr R G 1988 *Phys. Rev.* **B37** 785
34. Gonzalez C and Schlegel H B 1990 *J. Phys. Chem.* **94** 5523
35. Miertus S, Scrocco E and Tomasi J 1981 *J. Chem. Phys.* **55** 117
36. Miertus S and Tomasi J 1982 *J. Chem. Phys.* **65** 239
37. Frisch M J, Trucks G W, Schlegel H B, Scuseria G E, Robb M A, Cheeseman J R, Zakrzewski V G, Montgomery J A, Stratmann R E, Burant J C, Dapprich S, Millam J M, Daniels A D, Kudin K N, Strain M C, Farkas O, Tomasi J, Barone V, Cossi M, Cammi R, Mennucci B, Pomelli C, Adamo C, Clifford S, Ochterski J, Petersson G A, Ayala P Y, Cui Q, Morokuma K, Malick D K, Rabuck A D, Raghavachari K, Foresman J B, Cioslowski J, Ortiz J V, Stefanov B B, Liu G, Liashenko A, Piskorz P, Komaromi I, Gomperts R, Martin R L, Fox D J, Keith T, Al-Laham M A, Peng C Y, Nanayakkara A, Gonzalez C, Challacombe M, Gill P M W., Johnson B G, Chen W, Wong M W, Andres J L, Gonzalez C, Head-Gordon M, Replogle E S and Pople J A 1998 *GAUSSIAN98*, Revision A.7; Gaussian Inc. Pittsburgh, PA